

Ultrafast optical study of spin wave resonance and relaxation in a CoFe/PtMn/CoFe trilayer film

Y. H. Ren,^{1,a)} C. Wu,¹ Y. Gong,¹ C. Pettiford,² and Nian X. Sun²

¹*Physics and Astronomy, Hunter College of the City University of New York, 695 Park Avenue, New York, New York 10065, USA*

²*Electrical and Computer Engineering, Northeastern University, 409 Dana Research Center, 360 Huntington Avenue, Boston, Massachusetts 02115, USA*

(Presented 13 November 2008; received 23 September 2008; accepted 30 October 2008; published online 4 February 2009)

We report on our recent study of confined spin wave excitations in a 200 Å CoFe/PtMn/CoFe trilayer film by ultrafast Kerr-rotation experiments. Coherent magnetization precessions were generated and detected by subpicosecond laser pulses. Three precession modes are observed when a magnetic field is oriented in the film plane. The frequencies of two modes increase with the field, while one mode shows no field dependence. The modes are assigned to the exchange-dominated spin wave excitations and the nonhomogeneous dipole mode. We used a comprehensive model of the magnetic eigenmodes and their coupling to light to gain values of the exchange, bulk, and surface anisotropy constants. Further, we investigated spin wave relaxation as a function of the applied field. We calculated an effective damping constant for the uniform precession to be $\alpha \sim 0.012$. © 2009 American Institute of Physics. [DOI: [10.1063/1.3063675](https://doi.org/10.1063/1.3063675)]

Soft magnetic multilayer films have recently attracted a great deal of attention because of their potential applications in magnetic sensors and rf/microwave devices.^{1–3} As a result of the interfacial interaction and/or the exchange coupling, the sandwiched films show excellent magnetic softness with a uniaxial anisotropy field and a low coercivity.⁴ One such example is the Ru-seeded CoFe/PtMn/CoFe structure.^{5,6} The high moment ferromagnetic (FM) CoFe thin films couple strongly with antiferromagnetic (AFM) PtMn layer, rendering a low hard axis coercivity of 2–4 Oe and a significant enhancement of in-plane anisotropy of ~ 57 –123 Oe.

In order to get a better understanding of dynamical magnetic parameters of the exchange-coupled structures and therefore assess their technological potential, it is essential to investigate their low energy spin wave spectrum. The magnon spectrum at low frequencies can be determined and used to obtain the exchange and magnetic anisotropy parameters and the damping parameters if spin wave excitations are introduced via pulsed photoexcitation and the magnetization precessions and relaxation processes are studied on a picosecond time scale.^{7–10}

In this paper, we report on time-resolved pump-probe differential magnetic Kerr (DMK) measurements of magnetization dynamics in a 200 Å CoFe/PtMn/CoFe film grown on the seed layer Ru with CoFe compositions being Co 16 at. % Fe. Coherent magnetization precessions were generated and detected by subpicosecond laser pulses. We observed three precession modes with a magnetic field applied parallel to the easy axis direction. The frequencies of two modes increase with the field, while one mode shows no field dependence. The modes are assigned to the exchange-dominated spin wave excitations and the nonhomogeneous

dipole mode. We used a comprehensive model of the magnetic eigenmodes and their coupling to light, to gain values of the exchange, bulk, and surface anisotropy constants. In addition, we analyzed the magnetization relaxation dynamics of the CoFe/PtMn/CoFe sample. We obtained an effective damping constant of ~ 0.012 . The surface anisotropy contribution is found to be critical for understanding the magnetization dynamics.

The multilayer CoFe/PtMn/CoFe film was grown on a seed layer of Ru with CoFe film compositions being Co 16 at. % Fe, the details of which are reported elsewhere.⁵ The thickness of the FM CoFe layers is ~ 200 Å and that of the AFM layer is ~ 120 Å. The pump-probe DMK experiments in the CoFe/PtMn/CoFe film were performed at ~ 77 K in the Voigt geometry using a Ti-sapphire laser that provided ~ 70 fs pulses of central wavelength 780 nm at a repetition rate of 82 MHz. The energy of the pump pulse is ~ 10 nJ, while less than 1 nJ is used for the probe. The pump pulses induce coherent magnetic precessions modifying the reflection of the probe pulses that follow behind. The pump-induced shift in the polarization angle of the reflected probe field $\delta\theta$ was measured as a function of the time delay between the two pulses. Because scattering by spin-flip excitations is described by an antisymmetric tensor, the signature of a pure-spin magnetic precession is $\Delta E_R \perp E_R$ (or $\Delta R=0$), where ΔE_R is the pump-induced change in the field of the reflected probe beam and E_R is the reflected probe field when the pump is turned off. This selection rule was strictly obeyed in all our measurements.

The experimental results are summarized in Figs. 1 and 2. Figure 1 shows DMK data for the 200 Å thick CoFe trilayer sample after subtracting an exponentially decaying background. The oscillations are assigned to the precession of the magnetization around M_0 . We used linear prediction methods to fit the time-domain data and, as shown in the

^{a)}Electronic mail: yre@hunter.cuny.edu.

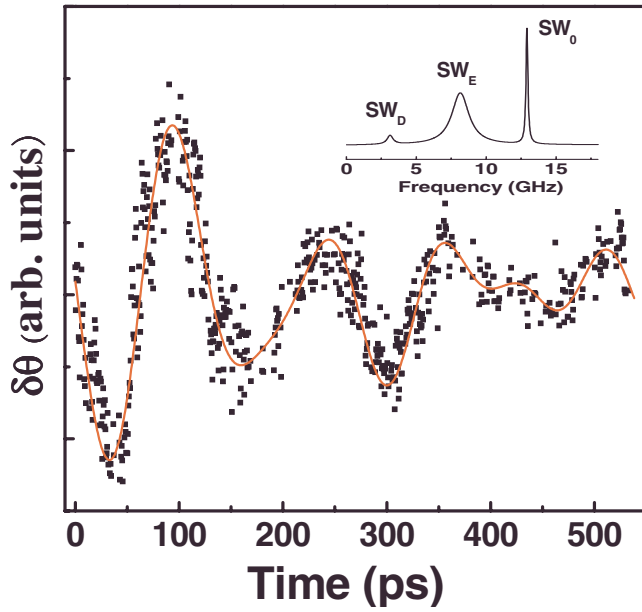


FIG. 1. (Color online) Voigt-geometry DMK data for the 200 Å CoFe/PtMn/CoFe film (solid square) at 320 Oe. The red curve is the linear prediction fit. The inset shows the Fourier transform of the fit.

inset in Fig. 1, the Fourier transform of the fit reveals three modes, which are assigned as SW_E , SW_0 , and SW_D . While SW_E and SW_0 refer to the surface and bulk exchange-dominated spin wave modes, the observation of SW_D , the nonhomogeneous dipole mode, is due to the finite penetration depth of the pump pulses. The three modes were observed in the DMK spectra of all the magnetic fields and show little dependence of thickness of the samples. The frequencies of the modes are plotted as a function of the applied magnetic field in Fig. 2, together with ferromagnetic resonance (FMR) results.

Unlike the sharp selection rules of Raman type observed in probe scattering,^{11,12} we find that the strength of the oscillations is nearly the same for pump pulses of arbitrary circu-

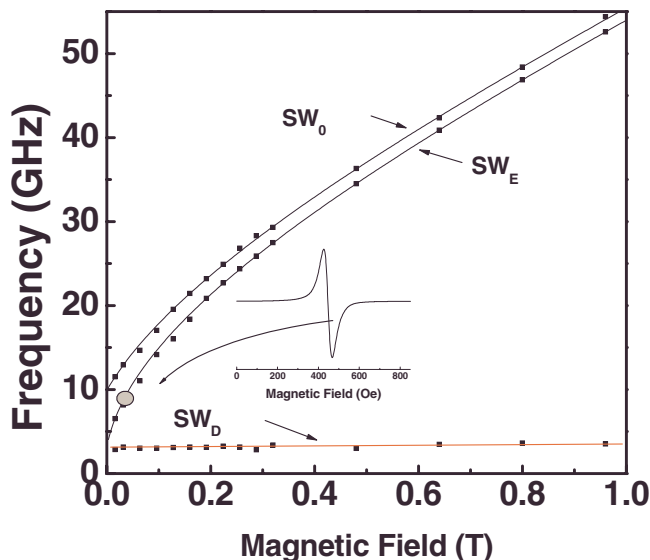


FIG. 2. (Color online) Measured magnetic-field dependence of the precession mode frequencies. The inset is the FMR spectrum and the solid lines show the fits.

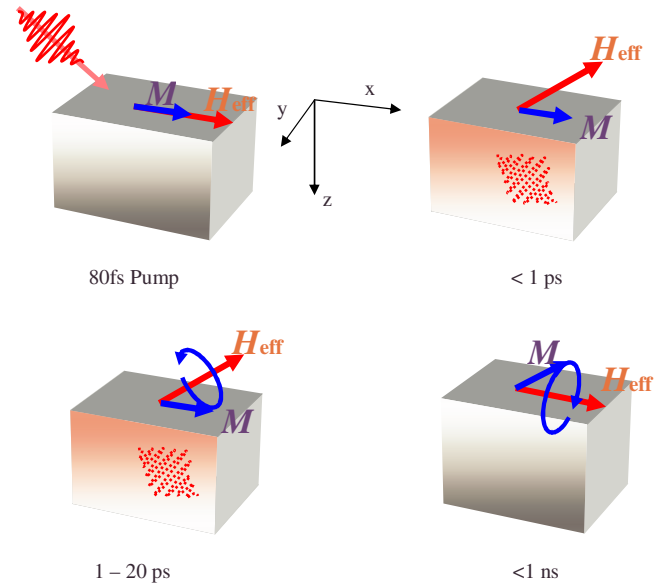


FIG. 3. (Color online) Schematics of the spin wave excitations in the pump-probe DMK experiments and the corresponding coordinate axis.

lar or linear polarization. The results point toward a relatively simple thermal origin relying on the temperature dependence of the anisotropy.¹⁰ A sudden deviation of the orientation of \mathbf{M}_0 is due to the temperature rise that follows the absorption of the light pulse. As shown in Fig. 3, the easy-axis orientation moves to a new orientation after the pulse hits. The orientation of the effective magnetic field shifts and the magnetization aligns with the new easy axis for a couple of picoseconds. The magnetization, already out of equilibrium, is not aligned with the effective magnetic field and starts to precess around the new easy axis with a tendency to align with the new effective field. The thermally induced anisotropy field pulse lasts no longer than a couple of picoseconds until electrons, phonons, and spins achieve thermal equilibrium. Once thermal equilibrium is established, the easy axis of the ferromagnet returns to the position from before excitation and the magnetization starts to precess around a constant effective field.

We use the Landau–Lifshitz–Gilbert equation to describe the motion of the magnetization \mathbf{M} .¹³ The eigenfrequencies of the magnetization precession are

$$\begin{aligned} \omega^2 = & \gamma^2 \left(H_0 + \frac{2K_A}{M_0} \right) \left[H_0 + 4\pi M_0 + 2M_0^{-1} (K_A - K_U) \right] \\ & \pm Dk^2 \gamma^2 \left\{ \left(H_0 + \frac{2K_A}{M_0} \right) + [H_0 + 4\pi M_0 \right. \\ & \left. + 2M_0^{-1} (K_A - K_U)] \right\} + \gamma^2 Dk^2, \end{aligned} \quad (1)$$

where the plus (minus) sign corresponds to the bulk-(surface)-like modes; K_U and K_A are the out-of-plane and in-plane anisotropy constants. The eigenmodes are selected by the conditions at the boundaries¹⁴ $\partial m_y / \partial z = 0$, $\frac{\partial \ln m_z}{\partial z} = -\frac{2K_S}{DM_0}$ at $z=L/2$ and $\partial \ln m_z / \partial z = 2K_f / DM_0$ at $z=-L/2$, where K_S and K_f are the surface and interface anisotropy constants, respectively. Here we have neglected the exchange bias field between the CoFe layer and the PtMn layer according to our FMR and vibrating-sample magnetometer (VSM) hysteresis results on the CoFe/PtMn/CoFe sample: H_{ei}

≤ 15 Oe. The interlayer exchange interaction between the CoFe layers is small due to their large separation.

The observation of the SW_E and SW_0 can be described by the coupling between magnetic precessions and probe pulses by the antisymmetric spin-flip Raman susceptibility, which is closely related to that for Faraday rotation.¹⁵ In the Voigt geometry, the scattered probe field associated with the m_y component of the precession is polarized along the z -axis and, therefore, gives no DMK signal. Using results for scattering by coherent vibrations,^{16,17} we get the following for m_z scattering:

$$\left(\nabla^2 - \frac{n_R^2}{c^2} \frac{\partial^2}{\partial t^2}\right)(e_x \pm ie_y) = \frac{4\pi\chi_M}{c^2} \frac{\partial^2}{\partial t^2} [m_z(z,t)(e_y \pm ie_x)], \quad (2)$$

where $e=(e_x, e_y, 0)$ is the probe electric field, n_R is the refractive index, and $\chi_M = \partial\chi^{(0)}/\partial M$ with $\chi^{(0)}$ representing the linear susceptibility. In our case, since the FM thickness is comparable to the penetration depth (~ 300 Å), we are able to observe both the homogeneous and inhomogeneous modes. For the homogeneous modes it can be shown that coherent scattering is equivalent to a slowly varying modulation of the refractive index,

$$\delta n_R(t) = \pm \left(\frac{2\pi\chi_M}{n_R L}\right) \int_{-L/2}^{L/2} m_z(z,t) dz \quad (3)$$

with different signs for the two senses of circular polarization. Except for the constant factors, this expression is identical to that describing FMR. We obtained that the amplitude of the DMK signal for a given precession $\delta\theta$ is proportional to $\langle m_y \rangle \langle m_z \rangle / \langle m_y^2 \rangle$. The amplitude shows a strong dependence of the magnetization profiles; therefore, of K_S and K_f , we can determine the surface and interface anisotropy parameters from the relative ratio between the amplitudes of SW_E and SW_0 . The solid lines in Fig. 2 show the fitting of the present DMK data using Eq. (1). We obtained $g=2.1$, the out-of-plane uniaxial anisotropy, $2K_U/M \sim -0.2$ T, the effective in-plane anisotropy, $2K_A/M \sim 0.01$ T, the effective demagnetization field, $4\pi M_{\text{eff}} \sim 2.1$ T, and the spin stiffness, $D \sim 451$ meV.Å². Our values for the magnetic anisotropies and spin stiffness are in fairly good agreement with those from the FMR and VSM measurements.^{5,6}

In addition to SW_E and SW_0 , SW_D with significantly smaller intensity also contributes to our time resolved spectra. This mode is independent of external field and has a constant frequency of 3.1 GHz. The small frequency implies the dipole origin of this mode. We attribute it to the so-called volume backscattered dipole mode. The excitation of the mode is due to the finite penetration depth of the pump beam, which launches thermal gradient inside the magnetic layers. The dispersion relation of the mode has been studied in detail in the Permalloy dots using Brillouin light scattering.^{18,19}

Further, we analyzed the magnetization relaxation dynamics of the CoFe/PtMn/CoFe sample. In time-resolved measurements, magnetic damping is determined by the char-

acteristic relaxation time τ of the amplitude of the magnetization precession. For the film samples with the magnetization mostly aligned in the in-plane direction, in the limit of small damping ($\alpha \ll 1$), the effective damping constant α for the uniform precession can be described by²⁰

$$\alpha \approx \left[\mu_0 \gamma \tau \left(H + \frac{4\pi M_{\text{eff}}}{2}\right)\right]^{-1}, \quad (4)$$

where the small effective in-plane anisotropy H_A has been neglected and H is the applied external magnetic field. By substituting the above parameters and the characteristic relaxation time, we obtained the effective damping constant as of ~ 0.012 .²¹

In summary, we performed pump-probe DMK experiments in the 200 Å trilayer CoFe/Pt/CoFe films. Three precession modes were observed in the Voigt geometry. The modes are assigned to the exchange-dominated spin wave excitations and the nonhomogeneous dipole mode. We developed a comprehensive model of the magnetic eigenmodes and their coupling to light to gain values of the effective magnetization and the exchange and bulk constants. The results are consistent with those from the FMR measurements. Moreover, we calculated the effective damping constant as ~ 0.012 .

- ¹M. Yamaguchi, S. Arakawa, H. Ohzeki, Y. Hayashi, and K. I. Arai, *IEEE Trans. Magn.* **28**, 3015 (1992).
- ²A. M. Crawford, D. Gardner, and S. X. Wang, *IEEE Trans. Magn.* **38**, 3168 (2002).
- ³B. Kuanr, Z. Celinski, and R. E. Camley, *Appl. Phys. Lett.* **83**, 3969 (2003).
- ⁴S. X. Wang, N. X. Sun, M. Yamaguchi, and S. Yabukami, *Nature (London)* **407**, 150 (2000).
- ⁵C. Pettiford, A. Zeltser, S. Z. D. Yoon, V. G. Harri, C. Vittoria, and N. X. Sun, *J. Appl. Phys.* **99**, 08C901 (2006).
- ⁶C. Wu, A. N. Khalfan, C. Pettiford, N. X. Sun, S. Greenbaum and Y. H. Ren, *J. Appl. Phys.* **103**, 07B525 (2008).
- ⁷E. Beaurepaire, J. Merle, A. Daunois, and J. Bigot, *Phys. Rev. Lett.* **76**, 4250 (1996).
- ⁸M. van Kampen, C. Jozsa, J. Kohlepp, P. LeClair, L. Lagae, W. de Jonge, and B. Koopmans, *Phys. Rev. Lett.* **88**, 227201 (2002).
- ⁹W. K. Hiebert, A. Stankiewicz, and M. R. Freeman, *Phys. Rev. Lett.* **79**, 1134 (1997).
- ¹⁰D. M. Wang, Y. H. Ren, X. Liu, J. K. Furdyna, M. Grimsditch, and R. Merlin, *Phys. Rev. B* **75**, 233308 (2007).
- ¹¹A. V. Kimel, A. Kirilyuk, and P. Usachev, *Nature (London)* **435**, 655 (2005).
- ¹²F. Hansteen, A. Kimel, A. Kirilyuk, and T. Rasing, *Phys. Rev. B* **73**, 014421 (2006).
- ¹³L. Landau and E. Lifshitz, *Phys. Z. Sowjetunion* **8**, 153 (1935).
- ¹⁴G. T. Rado and J. R. Weertman, *J. Phys. Chem. Solids* **11**, 315 (1959).
- ¹⁵W. Hayes and R. Loudon, *Scattering of Light by Crystals* (Wiley, New York, 1978).
- ¹⁶R. Merlin, *Solid State Commun.* **102**, 207 (1997).
- ¹⁷T. E. Stevens, J. Kuhl, and R. Merlin, *Phys. Rev. B* **65**, 144304 (2002).
- ¹⁸G. Gubbiotti, C. Carlotti, T. Okuno, T. Shinjo, F. Nizzoli, and R. Zivieri, *Phys. Rev. B* **68**, 184409 (2003).
- ¹⁹G. Gubbiotti, M. Kostylev, N. Sergeeva, M. Conti, G. Carlotti, T. Ono, A. Slavin, and A. Stashkevich, *Phys. Rev. B* **70**, 224422 (2004).
- ²⁰J. Walowski, M. D. Kaufmann, B. Lenk, and C. Hamann, J. McCord, and M. Müntenberg, *J. Phys. D* **41**, 164016 (2008).
- ²¹Within the ansatz given by Gilbert, the damping constant α is assumed to be field-independent. Here, the damping constant is calculated by averaging over magnetic field region where the damping is mostly constant, say $H > 700$ Oe.